J Geophys (1983) 53: 34–41

Journal of Geophysics

Gravity Interpretation of Two Dimensional Fault Structures Using Hilbert Transforms

N. Sundararajan, N.L. Mohan, and S.V. Seshagiri Rao

Centre of Exploration Geophysics, Osmania University, Hyderabad-500007, India

Abstract. The Hilbert Transform of the second order horizontal gradient of the gravity effect of a two dimensional dipping fault is derived. Using the derivatives of the horizontal gradient of the gravity effect and the Hilbert Transform, the parameters of the dipping fault, namely the dip, the depths to the top and bottom and the density contrast, are obtained. The gravity effect of the vertical fault has also been analysed treating it as a particular case of the dipping fault. The validity of the method is exemplified with theoretical and field examples in either cases.

Key words: Gravity anomaly – Horizontal derivative – Fault structure – Fourier transform – Discrete Hilbert transform – Points of intersection – Density contrast

Introduction

In recent years, Hilbert transformation techniques (Nabighian, 1972; Stanley and Green, 1976; and Stanley, 1977) have assumed importance in the quantitative interpretation of gravity and magnetic data. Nabighian's (1972) work was confined to the transformation of vertical gradients (vertical magnetic field) into horizontal gradients (horizontal magnetic field) and vice-versa with the help of the Hilbert transform. But Mohan et al. (1982) have devised a novel interpretation technique making use of the Hilbert transform to analyse vertical magnetic anomalies due to some two dimensional bodies, through which the parameters of the causative body are determined by means of simple mathematical expressions. The very same approach has been extended in the present paper for determining the parameters of two dimensional fault structures. Since the gravity effect and its Hilbert transformation are in the space domain, the kind of assumptions which are necessary in frequency domain techniques, (Bhimasankaram et al., 1977) are no longer required.

Gravity Effect of a Dipping Fault

For a semi infinite dipping fault block of finite throw (Fig. 1a), the gravity effect is given by (Jung, 1961):

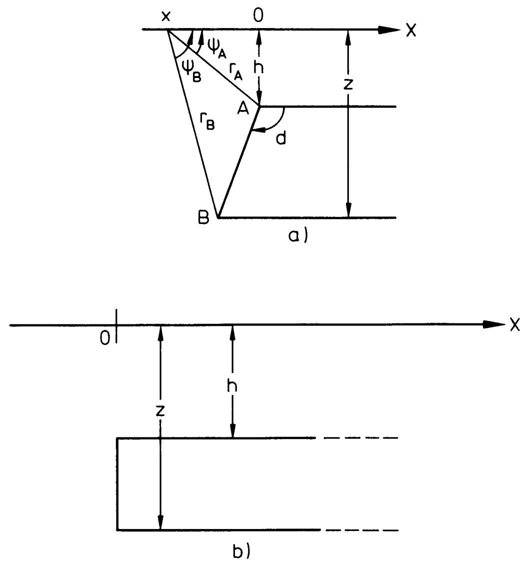

Fig. 1. a Geometry of the two dimensional dipping fault. **b** Geometry of the two dimensional vertical fault

$$g(x) = 2G\sigma \sin d [(x + h \cot d) \cdot \sin d \{\sin d \ln(r_B/r_A) - \cos d(\varphi_B - \varphi_A)\} + (Z\varphi_B - h\varphi_A)] \quad (1)$$

where

G – is the gravitational constant.
σ – is the density contrast.
d – is the dip of the fault.
h – is the depth to the top of the fault.
and
Z – is the depth to the bottom of the fault.

Differentiating Eq. (1) with respect to x twice, we obtain,

$$g''(x) = 2G\sigma \sin d \left[\frac{h \cos d - x \sin d}{r_A^2} - \frac{(2Z-h)\cos d - x \sin d}{r_B^2}\right]. \quad (2)$$

Equation (2) can be rewritten as,

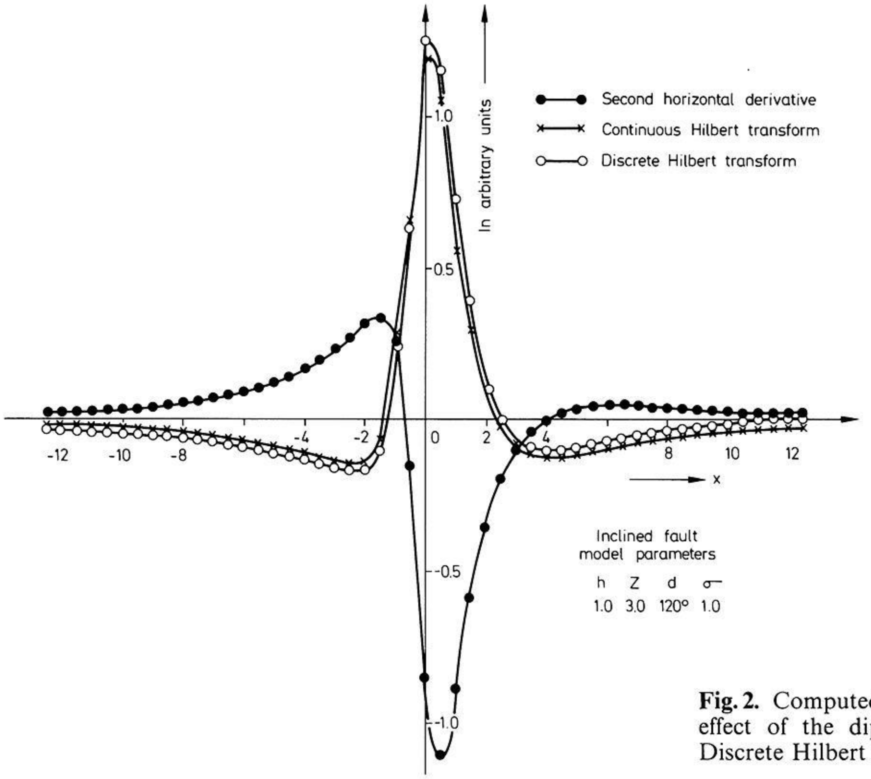

Fig. 2. Computed second horizontal gradient of the gravity effect of the dipping fault, the Hilbert transform and the Discrete Hilbert transform. (Model I)

$$g''(x)=2G\sigma\sin d\left[\frac{h\cos d-x\sin d}{x^2+h^2}+\frac{(x-D)\sin d-Z\cos d}{(x-D)^2+Z^2}\right] \quad (3)$$

where $D=(Z-h)\cot d$.

The Fourier transform of $g''(x)$ is given by,

$$F(\omega)=\int_{-\infty}^{\infty} g''(x)\,e^{-i\omega x}\,dx. \quad (4)$$

Substituting for $g''(x)$ from Eq. (3) in Eq. (4) and evaluating the integral, the real and imaginary components of the Fourier transform are obtained as:

$$\operatorname{Re}F(\omega)=2\pi G\sigma\sin d\,[e^{-\omega h}\cos d-\cos(d-\omega D)\,e^{-\omega Z}] \quad (5)$$

and

$$\operatorname{Im}F(\omega)=2\pi G\sigma\sin d\,[e^{-\omega h}\sin d-\sin(d-\omega D)\,e^{-\omega Z}]. \quad (6)$$

Hilbert Transform

The Hilbert transform of $g''(x)$ is defined as (Thomas, 1969):

$$H(x)=\frac{1}{\pi}\int_{0}^{\infty}[\operatorname{Im}F(\omega)\cos\omega x-\operatorname{Re}F(\omega)\sin\omega x]\,d\omega. \quad (7)$$

Substituting Eqs. (5) and (6) in Eq. (7), and then integrating, the Hilbert transform is obtained as,

$$H(x)=2G\sigma\sin d\left[\frac{h\sin d-x\cos d}{x^2+h^2}+\frac{(x-D)\cos d-Z\sin d}{(x-D)^2+Z^2}\right]. \quad (8)$$

Evaluation of Parameters

Following Nabighian (1972) we determine the origin by considering the maxima of,

$$A(x)=\sqrt{[g''(x)]^2+[H(x)]^2}. \quad (9)$$

Then the approximate dip of the fault block is determined (see Appendix) using the relation,

$$d=\cot^{-1}\left[\frac{g''(0)}{H(0)}\right]. \quad (10)$$

For $g''(0)=0$, d becomes 90 degrees which is the case of a vertical fault. The graphs of the second horizontal derivative of the gravity effect of an inclined fault block $g''(x)$, and its Hilbert transform, $H(x)$, are found to intersect on either side of the origin (Figs. 2 and 3).

If the abscissa of the points of intersection are x_1 and x_2 then,

$$g''(x_{1,2})=H(x_{1,2})$$

(i.e.)

$$x_1^2(h-Z-D)+x_1(D^2+Z^2-h^2-2hD)=Zh^2-hZ^2-h^2D-hD^2 \quad (11)$$

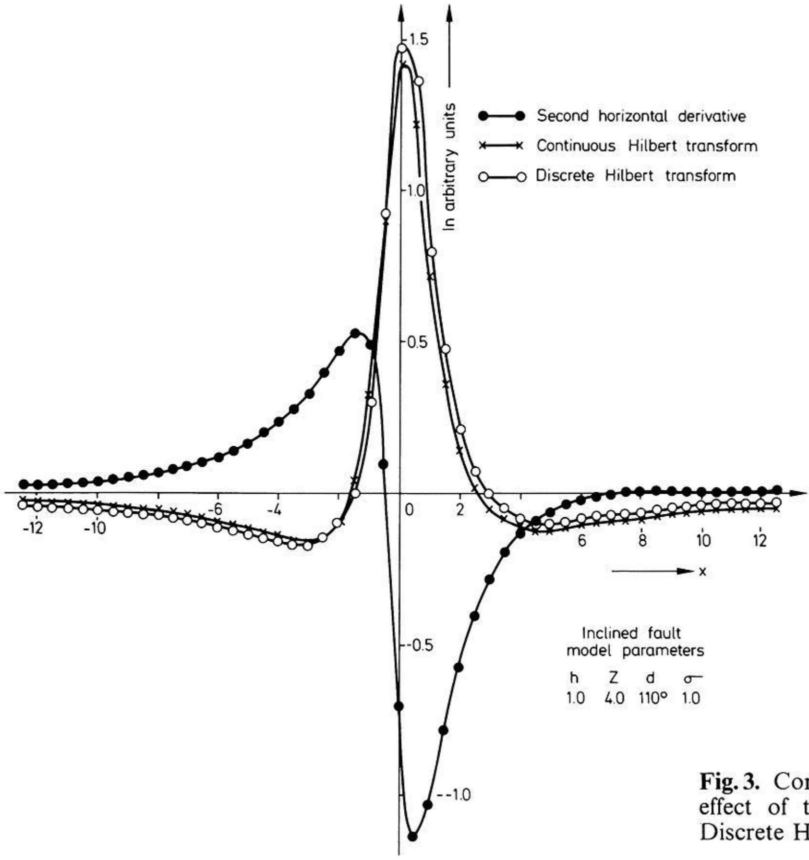

Fig. 3. Computed second horizontal gradient of the gravity effect of the dipping fault, the Hilbert transform and the Discrete Hilbert transform. (Model II)

and

$$x_2^2(h-Z-D)+x_2(D^2+Z^2-h^2-2hD)$$
$$=Zh^2-hZ^2-h^2D-hD^2. \tag{12}$$

Solving equations (11) and (12), the depths to the top h, and bottom Z are obtained as,

$$h=\frac{(x_1+x_2)\pm\sqrt{(x_1+x_2)^2+4x_1x_2(K_2+K_3)}}{2(K_2+K_3)} \tag{13}$$

and

$$Z=\frac{K_3h^2-x_1x_2}{K_1h} \tag{14}$$

where

$$K_1=\frac{(1+P^2)}{1-P},$$

$$K_2=\frac{1+2P-P^2}{1-P},$$

$$K_3=\frac{P(1+P)}{1-P}$$

and

$$P=\cot d.$$

Finally the density contrast σ is determined from,

$$\sigma=\frac{1}{2G\sin d}\sqrt{\frac{[g''(0)]^2+[H(0)]^2}{A+B+C}} \tag{15}$$

where

$$A=\frac{1}{h^2},$$

$$B=\frac{D^2+Z^2+4DZ\cos d\sin d}{(Z^2+D^2)^2},$$

$$C=-\frac{2(Z+2D\sin d\cos d)}{h(Z^2+D^2)}.$$

Thus, the above analysis facilitates the determination of all the parameters of the dipping fault.

Vertical Fault

The semi infinite vertical fault block (Fig. 1b) is just a particular case of the dipping fault with d assuming the value $\pi/2$.

Correspondingly the second horizontal derivative of the vertical fault and its Hilbert transform are obtained by substituting $d=\pi/2$ in Eqs. (3) and (8).

Thus,

$$g_1''(x)=2G\sigma\left[\frac{x}{x^2+Z^2}-\frac{x}{x^2+h^2}\right] \tag{16}$$

and

$$H_1(x)=2G\sigma\left[\frac{h}{x^2+h^2}-\frac{Z}{x^2+Z^2}\right]. \tag{17}$$

Table 1. Theoretical Examples (* In arbitrary units)

	Parameters	d	h^*	Z^*	σ^*
Dipping fault					
Model I	Assumed values	120.0°	1.00	3.00	1.00
	Evaluated values	123.8°	1.11	3.14	1.03
Model II	Assumed values	110.0°	1.00	4.00	1.00
	Evaluated values	114.6°	0.97	3.90	1.11
Vertical fault					
Model I	Assumed values	-	0.50	1.00	1.00
	Evaluated values	-	0.56	0.99	1.28
Model II	Assumed values	-	1.00	3.00	1.00
	Evaluated values	-	1.00	2.71	0.95

Evaluation of Parameters

As in the earlier case the graphs of $g_1''(x)$ and $H_1(x)$ are found to intersect on either side of the origin (Figs. 4 and 5). The parametric evaluation in the case of a vertical fault can be made simple by substituting $d=\pi/2$ in Eqs. (13), (14) and (15) which yield the depth to the top and bottom and the density contrast as follows:

$$h=\frac{(x_1+x_2)\pm\sqrt{(x_1+x_2)^2+4x_1x_2}}{2}, \tag{18}$$

$$Z=\frac{-x_1x_2}{h} \tag{19}$$

and

$$\sigma=\frac{hZ\sqrt{[g''(0)]^2+[H(0)]^2}}{2G(Z-h)}. \tag{20}$$

Theoretical Examples

The theoretical procedures developed earlier as expressions of continuous variables can be made applicable to the field data which is discrete, by using the Discrete Fourier Transform (DFT) and the Discrete Hilbert Transform (DHT).

The real and imaginary components of the DFT are given by (Gold and Radar, 1969),

$$\operatorname{Re}F(n\omega_0)=\sum_{l=0}^{N-1} g''(l\cdot\Delta x)\cos(n\omega_0\cdot l\cdot\Delta x) \tag{21}$$

and

$$\operatorname{Im}F(n\omega_0)=\sum_{l=0}^{N-1} g''(l\cdot\Delta x)\sin(n\omega_0\cdot l\Delta x). \tag{22}$$

The discrete Hilbert Transform is defined as,

$$H(l\cdot\Delta x)=\frac{1}{\pi}\left[\sum_{n=0}^{\frac{N}{2}-1}\operatorname{Im}F(n\omega_0)\cos(n\omega_0\cdot l\Delta x)-\sum_{n=0}^{\frac{N}{2}-1}\operatorname{Re}F(n\omega_0)\sin(n\omega_0\cdot l\Delta x)\right]. \tag{23}$$

Where $\omega_0=2\pi/N\cdot\Delta x$ (radians per unit length) is the fundamental frequency, Δx is the station spacing and N is the total number of observed values.

Dipping Fault

Two theoretical models (Table 1) are analysed to examine the applicability of the procedure. With the help of Eqs. (3) and (8), the second horizontal derivative of the gravity effect and its Hilbert transform are computed in each case and shown in Figs. (2) and (3). The Discrete Hilbert Transform, $H(l\cdot\Delta x)$, is also computed in each case using (23) and they are also shown in the same Figures.

Using the Eqs. (10), (13), (14) and (15) the parameters, namely the dip d, the depth to the top h, the depth to the bottom Z and the density contrast σ are evaluated and presented (Table 1).

Vertical Fault

In the case of a vertical fault also, two theoretical models are computed using the corresponding equations and are shown in Figs. 4 and 5. The parameters of the causative body are evaluated using the procedure given for the vertical fault, and are presented in Table 1.

Field Examples

Dipping Fault

A profile of residual Bouger gravity anomaly (Fig. 6) across the Garber structure, Garber County, Oklahoma (Grant and West, 1965) is considered for interpretation. The entire profile is digitized into 64 equal parts such that it yields a station spacing of 121 m. The second horizontal derivative of the anomaly is computed numerically, and smoothed. Using an FFT algorithm the real and imaginary components of the DFT are computed and then the DHT is computed and plotted with the second horizontal derivative of the anomaly (Fig. 7). It is seen that these two curves intersect at $x_1=20.0$ and $x_2=-2.9$. The parameters of the causative body are evaluated and compared with that of Grant and West (Table 2).

Vertical Fault

Gravity data collected over a fault structure near Adilabad (at latitude 19°42′ N and longitude 78°33′ E), Andhra Pradesh, India, has been analysed (Fig. 8). From the shape of the anomaly it is assumed to be a vertical fault. The area of investigation forms a part of

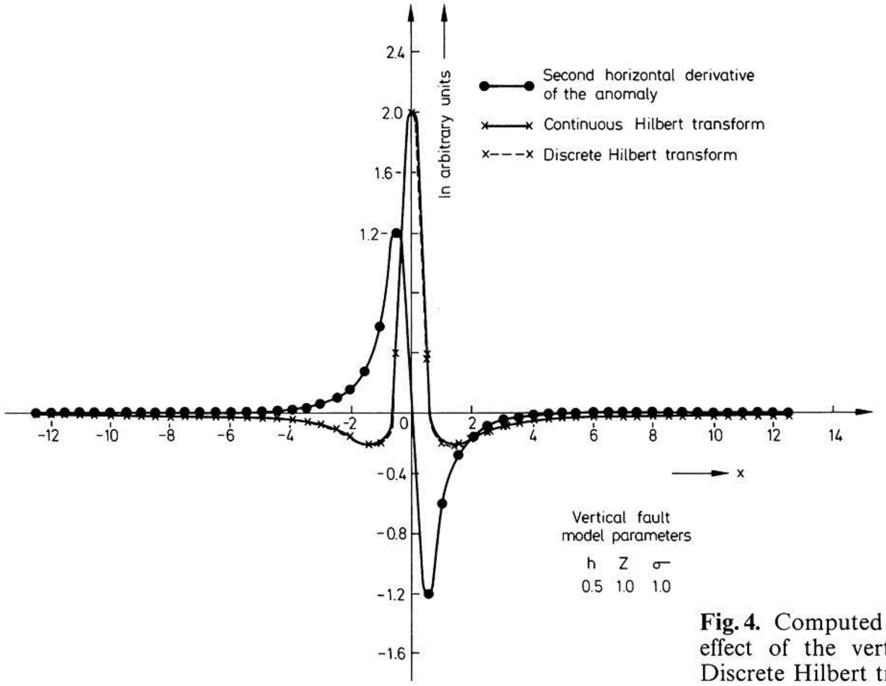

Fig. 4. Computed second horizontal gradient of the gravity effect of the vertical fault, the Hilbert transform and the Discrete Hilbert transform. (Model I)

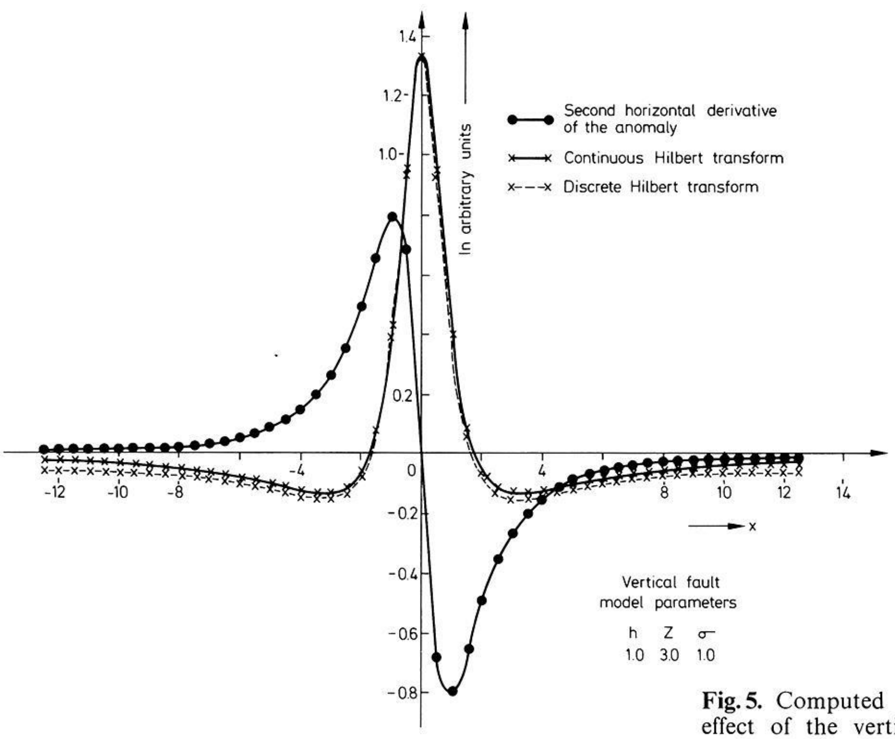

Fig. 5. Computed second horizontal gradient of the gravity effect of the vertical fault, the Hilbert transform and the Discrete Hilbert transform. (Model II)

the Penganga basin of precambrian sedimentary formation. It consists of two successions of alternating limestones and shales with basal quartzites. The stratigraphy sequence is as follows:

		....
		Shale[2]
		Limestone[2]
Precambrian sedimentaries	Penganga group	Shale Limestone Quartzite
		-Non-confirmity -

The length of the profile considered is 6.4 km and the station interval is 100 m. The computed second horizontal derivative of the anomaly and its DHT are

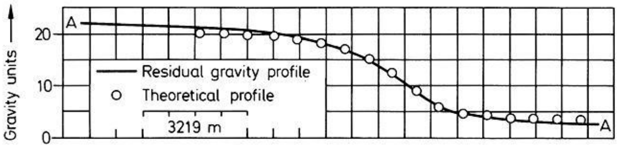

Fig. 6. Bouger gravity anomaly across the Garber structure, Garber County, Oklahoma

Table 2. Field Example (Dipping fault)

Parameters	d	h	Z	σ
Hilbert transform method	73.5°	327 m	2816 m	17.6 kg/m^3
Grant and West method	50°–70°	366 m	2804 to 4328 m	16.0 kg/m^3 to 22.0

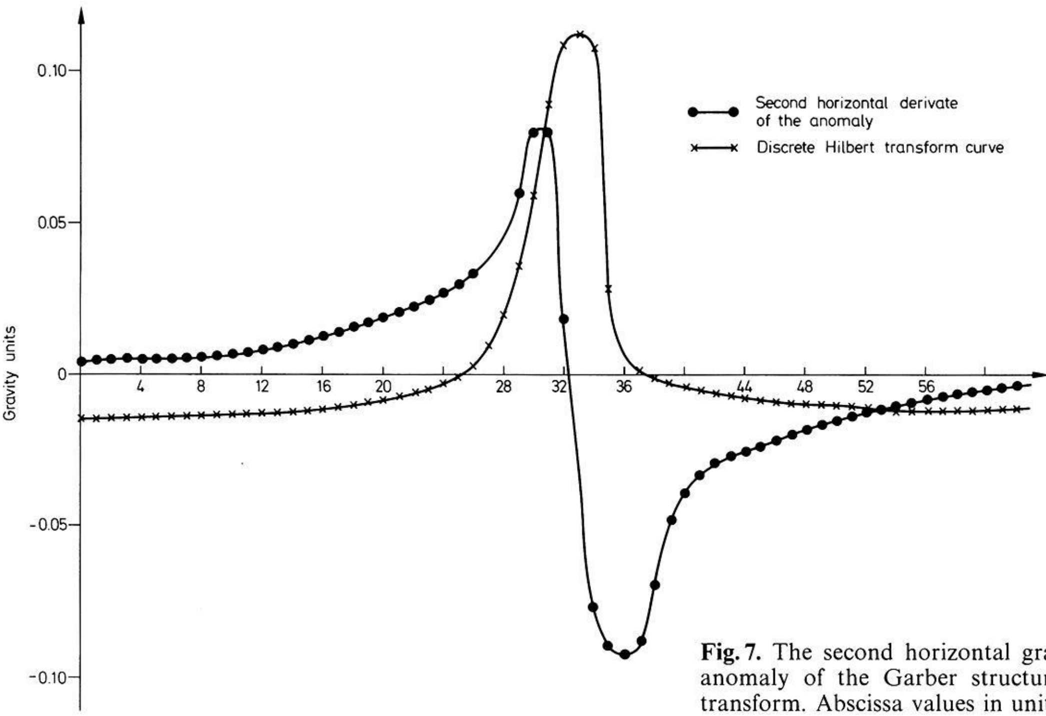

Fig. 7. The second horizontal gradient of the Bouger gravity anomaly of the Garber structure and the Discrete Hilbert transform. Abscissa values in units of 121 m

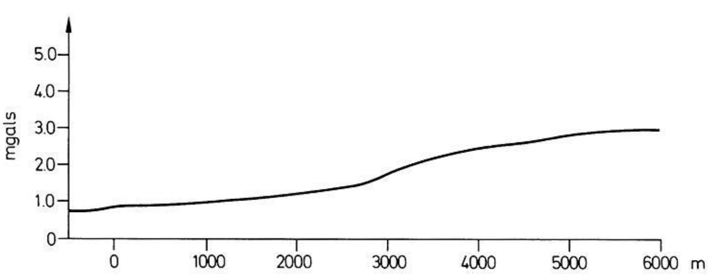

Fig. 8. Gravity anomaly over a vertical fault near Adilabad, Andhra Pradesh, India

plotted and shown (Fig. 9). It is observed that these two curves intersect at $x_1 = 7.6$ and $x_2 = -1.2$. Using the procedure detailed in the text, the results obtained are presented in Table 3.

Discussion

In this method differentiation of $g(x)$ with respect to x introduces a certain amount of error, consequently the Hilbert transform $H(x)$ is affected. The computation of the discrete Hilbert transform is further affected while taking the Fourier transform and its value depends upon the FFT algorithm. The sampling distances and the sampling rate used to digitize the measured potential gradients play an important role in minimising errors. It may be mentioned here that differentiation may be carried out effectively and more accurately in the frequency domain where, controlled by a dense sampling rate, the errors may be reduced sufficiently to obtain a reliable second derivative profile.

It may be pointed that the amount of error in the evaluation of parameters depends on the measurement of the gravity field and the computation of derivatives. We presume that an error of 0.1 units has been made in the measurement of $g(x)$ and the combined gradient value can be expressed as follows:

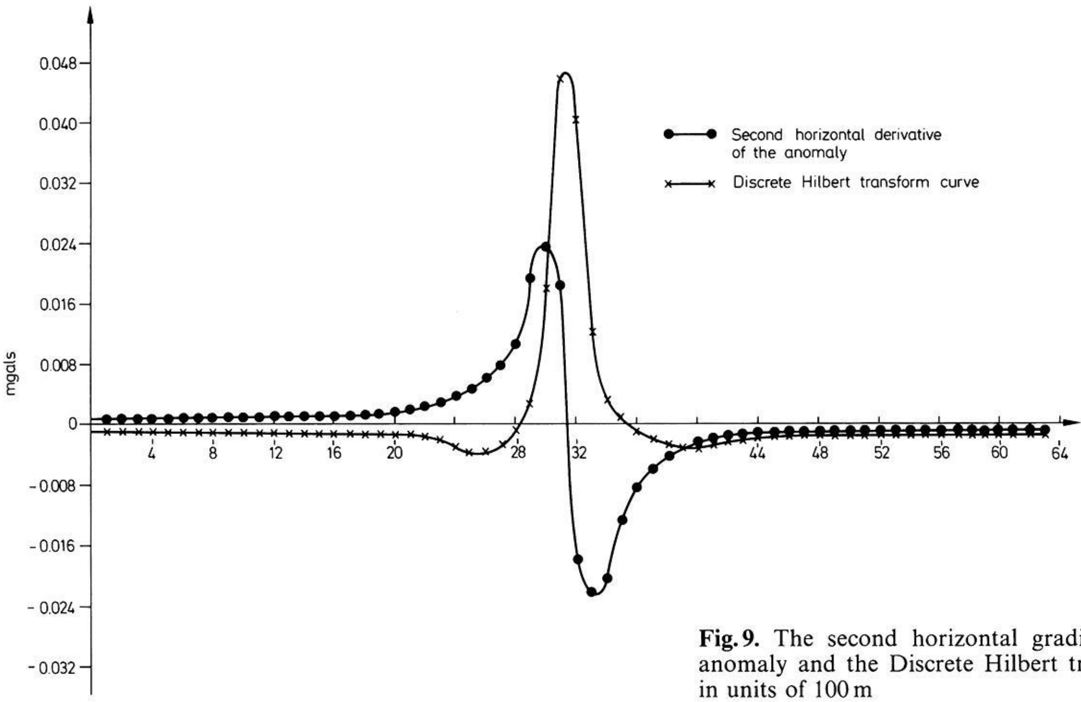

Fig. 9. The second horizontal gradient of the vertical fault anomaly and the Discrete Hilbert transform. Abscissa values in units of 100 m

Table 3. Field Example (Vertical fault)

Parameters	h	Z	σ
Hilbert transform method	214 m	426 m	122.2 kg/m^3

$g(x) = g(x) + 0.1\, g(x)$.

The Fourier transform of the above relation can be written as,

$$F(\omega) = F\left[\frac{d^2}{dx^2}\{g(x)\} + \frac{d^2}{dx^2}\{0.1\, g(x)\}\right]$$
$$= 1.1\, F[g''(x)].$$

Consequently, the Hilbert transform can be written as:

$$H(x) = H[1.1\, F\{g''(x)\}] + \varepsilon$$

where ε is a small amount of error introduced during the computation of Hilbert transform.

Hence, it is seen that the error in calculating the dip of the fault structure is

$$d = \tan^{-1}\left[\frac{1.1\, H(0) + \varepsilon}{1.1\, g''(0)}\right].$$

Therefore, it could be concluded that when $\varepsilon \to 0$, the dip of the fault is affected little by errors in the measurement and computation of the gravity field. However, the approximation made in determining the dip affects the subsequent evaluation of other parameters.

Appendix

At $x = 0$, the Eqs. (3) and (8) reduce to,

$$g''(0) = 2G\sigma \cdot \sin d\left[\cos d\left(\frac{1}{h} - \frac{Z}{D^2 + Z^2}\right) - \frac{D \cdot \sin d}{D^2 + Z^2}\right], \quad \text{(A.1)}$$

$$H(0) = 2G\sigma \cdot \sin d\left[\sin d\left(\frac{1}{h} - \frac{Z}{D^2 + Z^2}\right) - \frac{D \cdot \cos d}{D^2 + Z^2}\right]. \quad \text{(A.2)}$$

From Eqs. (A.1) and (A.2) we have,

$$\frac{g''(0)}{H(0)} = \frac{M \cdot \cot d - N}{M - N \cdot \cot d}. \quad \text{(A.3)}$$

Where,

$$M = \left(\frac{1}{h} - \frac{Z}{D^2 + Z^2}\right)$$

and

$$N = \frac{D}{D^2 + Z^2}.$$

For large values of Z, N approaches zero. So for many practical purposes, Eq. A-3 can be approximated to

$$\cot d = \frac{g''(0)}{H(0)}.$$

Acknowledgements. The authors thank the referees for their useful suggestions. Our thanks are also due to Professor M.S. Vijaya Raghava, Messrs. P.V. Harinath Baba and V. Veerabhadrappa, Centre of Exploration Geophysics, Osmania University, Hyderabad for providing the field data from the Adilabad area. Also one of the authors (N. Sundararajan) is grateful to the Council of Scientific and Industrial Research, Government of India for the financial help received. N.L. Mohan records his thanks to UGC for the financial grant.

References

Bhimasankaram, V.L.S., Mohan, N.L., Seshagiri Rao, S.V.: Analysis of the gravity effect of two dimensional trapezoidal prisms using Fourier Transform. Geophysical Prospecting, **35**, 334–341, 1977

Gold, B., Rader, C.M.: Digital processing of signals. New York: McGraw-Hill Co. 1969

Grant, F.S., West, G.F.: Interpretation theory in applied Geophysics. New York: McGraw-Hill Book Company 1965

Jung, K.: Schwerkraftverfahren in der angewandten Geophysik. Geest and Portig, 1961

Mohan, N.L., Sundararajan, N., Seshagiri Rao, S.V.: Interpretation of some two dimensional magnetic bodies using Hilbert transforms. Geophysics **47**, 376–387, 1982

Nabighian, I.N.: The analytic signal of two dimensional magnetic bodies with polygonal cross section, its properties and use for automated anomaly interpretation. Geophysics **37**, 507–512, 1972

Stanley, J.M., Green, R.: Gravity gradients and the interpretation of the truncated plate. Geophysics **41**, 1270–1276, 1976

Stanley, J.M.: Simplified gravity interpretation by gradients – The geological contact. Geophysics **42**, 1230–1235, 1977

Thomas, J.B.: An introduction to statistical communication theory. New York: John-Wiley and Sons, Inc. 1969

Received October 1, 1980; Revised version December 10, 1982; Accepted March 30, 1983